

# Water on Salt: An Infrared Study of Adsorbed H<sub>2</sub>O on NaCl(100) under Ambient Conditions

Steven J. Peters and George E. Ewing\*

Department of Chemistry, Indiana University, Bloomington, Indiana 47405

Received: August 28, 1997; In Final Form: October 1, 1997<sup>®</sup>

Using infrared spectroscopy, we were able to determine that water, under ambient conditions, adsorbs onto the surface of NaCl(100) into a liquidlike thin film. Photometric methods allowed coverages to be monitored from near  $\Theta = 0.1$  (0.1 monolayer) to  $\Theta = 3$ . The shifting band center of the  $\text{—OH}$  stretching region suggests changing hydrogen-bonding environments with coverage. In the submonolayer region, water–surface bonds are favored over water–water hydrogen bonds. Thin film coverages near  $\Theta = 2$  produce spectra essentially indistinguishable from that of a saturated salt solution suggesting a liquidlike hydrogen-bonded network. This thin film can be reversibly removed from the NaCl(100) surface. However, at coverages near  $\Theta = 3$ , dissolution begins and the salt surface becomes visibly damaged. Isotherms measured at 12 and 24 °C allowed the determination of the isosteric heat of adsorption. This heat of adsorption for coverages near  $\Theta = 2$  is close to that of the heat of condensation of liquid water, again suggesting that the thin film is liquidlike. A model for thin film water growth on NaCl(100) under ambient and cryogenic conditions is proposed.

## Introduction

“At Gerra, a town of Arabia, the walls and houses are made of blocks of salt cemented with water”; so wrote Roman naturalist, Pliny the Elder, in the first century A.D.<sup>1</sup> Blocks of salt, as a building material, would not fare so well in a humid climate where, at a relative humidity (RH) of 75% and temperature of 25 °C, droplets of brine would form on its sides as the process of dissolution (deliquescence) begins.<sup>2</sup> As we shall see, even under arid conditions of 30% RH, a monolayer of water forms on the NaCl(100) face, even though dissolution has not yet started. We seek an understanding of the structure of the adsorbed water and a mechanism of the dissolution process.

Under ambient conditions, a thin film of water coats many surfaces. This film can participate in heterogeneous transformations of solids such as rusting or corrosion.<sup>3</sup> Of relevance to environmental chemistry, it has become apparent that a film of water on the surface of salt from the sea plays an important role in its heterogeneous chemistry.<sup>4–6</sup> Adsorption of water to aerosol particles is the prelude to nucleation or cloud formation.<sup>7</sup> Other physical processes involving water films include adhesion, lubrication, and wetting.<sup>8–11</sup> Yet despite their importance to many processes in chemistry, biology, geology, physics, and meteorology, an understanding of the properties of water thin films, at the molecular level, is largely missing. How many molecular layers make up the thin film? What is its hydrogen-bonding arrangement? Is it best described as a liquid or solid? We provide answers to questions of this type by the spectroscopic study of water thin films under ambient conditions on a model substrate: the NaCl(100) surface.

One of the earliest studies of the water adlayer on NaCl(100) was performed by Hucher et al.<sup>12</sup> using electrical conductivity and transmission electron microscopy (TEM). Electrical conductivity was measured between two stripes of silver painted on the air cleaved NaCl(100) face. Three distinct regions of surface conductivity were found that describe the development

of the water adlayer. Below 40% RH (12 mbar at 25 °C<sup>13</sup>), the first region exhibited an exponential growth in conductivity with pressure. They proposed that H<sup>+</sup> ions in the adsorbed layer act as current carriers. Between 40% and 50% RH, a more gentle increase in conductivity was measured. In this second region, solvated Na<sup>+</sup> ions were suggested to contribute to the surface conductivity. Beyond 50% RH, the conductivity rose abruptly with both Na<sup>+</sup> and Cl<sup>–</sup> ions proposed to act as charge carriers. TEM images of the dry cleaved surfaces revealed smooth (100) terraces interrupted by steps of atomic dimensions. Hucher et al. then explored the morphological changes by exposing the crystals to water vapor, waiting for equilibrium to be established, evacuating the system, and then interrogating the transformed surfaces by TEM. After exposure to 20% RH, their microscopy revealed that the occasional sharp intersections of steps on the surface become rounded, suggesting that, at low pressure, water tends to favor adsorption to these defect sites and induce annealing. Near 40% RH, the concentration of steps on the surface increased abruptly. Finally, for 75% RH, microcrystallites had formed on the surface by the process of dissolution followed by recrystallization. In these elegant experiments performed 30 years ago, the first direct evidence that water radically alters the surface of NaCl(100), even under somewhat dry conditions, was documented.

More recent studies have applied atomic force microscopy (AFM) to interrogate the surface of NaCl(100). Shluger et al.<sup>14</sup> identify steps and other defects on the surface and suggest that adsorbed water on the AFM interrogation tip may alter the (100) face. Groups at Chuo University<sup>15,16</sup> quantify the migration of steps as a function of relative humidity. Shindo et al.,<sup>16</sup> for example, observe no step migration below 40% RH but find movement setting in precipitously near 65% RH. These humidity markers for surface changes are qualitatively consistent with the observations of Hucher et al.<sup>12</sup> Dai et al.<sup>17</sup> employ an electrostatic noncontact mode with their AFM measurements to reduce the influence of the probe tip on the surface of NaCl(100). Above ~35% RH, they interpret their AFM images as being produced by a uniform layer of water, and surface steps are observed to evolve slowly. At ~73% RH, step structure

\* To whom correspondence should be addressed.

<sup>®</sup> Abstract published in *Advance ACS Abstracts*, November 15, 1997.

disappears with the onset of dissolution (deliquescence). As we shall see, the infrared results we present here are qualitatively consistent with these observations and fill in the picture of adlayer changes with relative humidity.

Ultrahigh-vacuum (UHV) conditions are required for the use of surface-sensitive techniques such as low-energy electron diffraction (LEED) and helium atom scattering (HAS) to explore the architecture of the water adlayer on NaCl(100). The low water vapor pressures needed, less than about  $10^{-6}$  mbar, in turn demand temperatures below  $-110$  °C.<sup>2</sup> Consequently, only solidlike adlayers are explored. Fölsch et al.<sup>18</sup> have used LEED to study the water structure on the NaCl(100) substrate. The scattering pattern they observed was consistent with an adlayer structure of a well-ordered ice-like  $c(2 \times 4)$  bilayer. This structure is similar to a layer found in ordinary  $I_h$  ice, except that the adsorbed bilayer is slightly distorted to achieve compatibility with the NaCl(100) lattice. This adlayer then contains two types of water molecules. The first is in the bottom half of the layer, where the electronegative oxygen atoms in the water molecules are electrostatically attracted to  $\text{Na}^+$  ions on the surface and are hydrogen bonded to water molecules in the top half. Water molecules in the top half of the layer are not in direct contact with the substrate. Bruch et al.<sup>19</sup> studied adsorption of water to NaCl(100) by HAS under similar temperature and pressure conditions. In their model, the NaCl(100) lattice accommodates a  $(1 \times 1)$  water monolayer. To arrange the dipoles favorably, they suggest that the water molecules lie flat against the surface. While the LEED<sup>18</sup> and HAS<sup>19</sup> investigations indicated an ordered 2D condensed phase, IR (infrared) interrogation of  $\text{D}_2\text{O}$  on NaCl(100) at temperatures near 150 K and  $10^{-9}$  mbar of water vapor showed no evidence for such a phase.<sup>20</sup>

Theoretical methods have also been used to determine the adlayer structure. Wassermann et al.<sup>21</sup> used molecular dynamics calculations to explore the orientation of the permanent water dipole moment as a function of coverage. According to their calculations, at  $\Theta < 0.5$ , the water dipoles are perpendicular to the surface. Beyond half a monolayer they found that the dipoles begin to tilt toward the surface to favor hydrogen bonding between water molecules. Their theoretical adlayer structure agrees with the  $c(2 \times 4)$  bilayer structure found by Fölsch et al.<sup>18</sup> Calculations by Bruch et al.<sup>19</sup> and Jug and Geudtner<sup>22</sup> tend to favor a  $(1 \times 1)$  layer with the dipoles (i.e., molecular axes) nearly parallel to the surface.

A possible reason for the discrepancies between the low-temperature structures is the different NaCl substrates. In the HAS studies, in situ cleaved NaCl(100) single crystals were used,<sup>19</sup> while epitaxial grown NaCl adlayers on a Ge(100) surface were employed in the LEED investigation.<sup>18</sup> Jug and Geudtner<sup>22</sup> calculated the energy difference between the  $c(2 \times 4)$  and the  $(1 \times 1)$  structures and found it to be only 0.4 kJ/mol. With such a small difference in energy, any subtle differences in the substrate might affect which structure is favored. Although the disagreement about the structure of water on NaCl(100) at low temperatures has not been resolved, we will see that these proposed structures need not have much bearing on the  $\text{H}_2\text{O}$  adlayer arrangement under ambient conditions.

Infrared spectroscopy is useful for determining the structure of molecules adsorbed to NaCl(100) surfaces since this technique is sensitive to the phase of water, i.e., gas, liquid, or solid. While diffraction and scattering methods provide information about the adlayer lattice symmetry and dimension, they do not reveal molecular orientation. Polarized IR studies can supply this information. This technique has been useful in uncovering

structures and to infer molecular bonding arrangements for  $\text{CO}$ ,<sup>23,24</sup>  $\text{CO}_2$ ,<sup>25,26</sup> and  $\text{CH}_4$ <sup>27</sup> on the surface of NaCl(100).

In this paper we explore thin film water on NaCl(100) under ambient conditions using IR spectroscopy that complements our preliminary report.<sup>28</sup> A structure for the water adlayer as well as its physical nature is proposed from analysis of the  $-\text{OH}$  stretching region. Isothermic heats of adsorption are inferred from isotherm data. Both the isotherm measurements and the spectroscopy are used in proposing a mechanism for the adlayer growth.

## Experimental Section

Two sets of experiments were designed to explore, by infrared spectroscopy, the adlayer structure of water on NaCl(100) single-crystal surfaces. In one set, the emphasis was to measure, by polarized infrared radiation, the molecular orientations within the adlayer. The other set used unpolarized infrared measurements over a variety of pressures and adlayer coverages at two temperatures. Isotherms were generated from these measurements.

Vibrational spectra were recorded with a Fourier transform infrared (FTIR) spectrometer (Nicolet Magna-IR 550 or Bruker IFS-66). A liquid nitrogen cooled MCT (mercury cadmium telluride) detector was used in the polarization experiments and a liquid nitrogen cooled InSb (indium antimonide) detector for the isotherm studies. The resolution was set at  $4\text{ cm}^{-1}$  with a frequency survey of the region from 4000 to  $2000\text{ cm}^{-1}$ . A background interferogram was collected with 8000 scans. The sample interferogram consisted of 1000 scans ( $\sim 20$  min). Both the background and sample interferograms were transformed with a triangle apodization function and  $2\times$  zero filling. Absorbance,  $A = \log(I_0/I)$ , was plotted as a function of wavenumber,  $\tilde{\nu}$ , using a single-beam sample spectrum,  $I$ , and the appropriate background,  $I_0$ . Peak-to-peak noise under these conditions was  $A = 5 \times 10^{-5}$ . Water vapor features, which can obscure absorbance by the adlayer, were reduced by purging the spectrometer and subtracting out a reference spectrum of water vapor that had been appropriately scaled. The integrated absorbance,  $\tilde{A} = \int_{\text{band}} \log(I_0/I) d\tilde{\nu}$ , was obtained by a numerical integration procedure.

For the polarization measurements, four parallelepipeds were prepared by cleaving, under a dry  $\text{N}_2$  gas purge, along the NaCl(100) faces of larger crystals (Harshaw Inc.). These crystals were placed in a stainless steel sample holder and subsequently enclosed in a miniature ( $\sim 3\text{ cm}^3$ ) stainless steel UHV chamber (MDC Corps.). The small size of the chamber was necessary to minimize interfering water vapor absorbances. A schematic of the chamber and the orientation of the crystals is shown in Figure 1a. Silicon windows (Insulator Seal Inc.) were chosen to seal the chamber because they are transparent throughout most of the mid-infrared and are hydrophobic. The chamber was pumped by an ion pump (Varian) to a base pressure of  $< 1 \times 10^{-8}$  mbar. Both the chamber and the crystals were baked, prior to the start of the experiment, at  $130$  °C for 24 h. We have shown elsewhere that these procedures lead to clean well-defined NaCl(100) faces that can accept ordered adsorbed monolayers.<sup>23,25</sup> After cooling to  $22$  °C, water vapor was admitted, and the system was studied by transmission infrared spectroscopy. The water vapor was obtained from a liquid sample (Sigma, HPLC grade) that was degassed by four successive freeze–pump–thaw cycles. The infrared beam from the spectrophotometer passed directly through all four crystals, each canted at a  $45^\circ$  angle to the incident light, so that eight NaCl(100) faces were interrogated. Upon exiting the UHV chamber, the infrared beam passed through a polarizer (Molec-

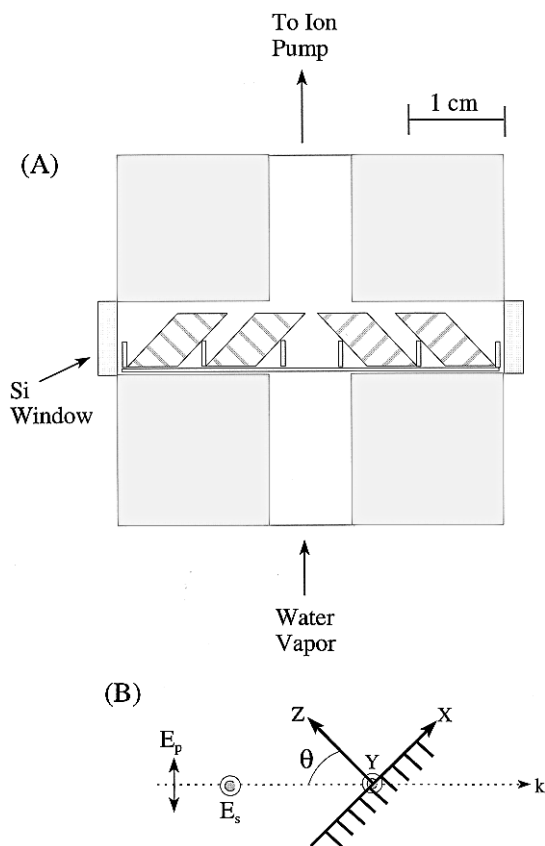


**Figure 1.** (a) Cross section of UHV chamber used in polarized FTIR experiments. (b) Orthographic projection showing the direction of propagation,  $k$ , and the electric field direction for  $E_p$ - and  $E_s$ -polarized light. The Z axis is perpendicular to the NaCl(100) surface; the X and Y axes point along [100] directions.

tron), and  $E_s$  spectra (the electric vector polarized perpendicular to the plane of incidence) and  $E_p$  spectra (polarized in the plane of incidence) were collected. These polarizations are depicted in Figure 1b.

For spectroscopic measurements as a function of temperature and pressure, 10 crystals ( $1.5 \times 1.5 \times 1.0$  cm) cleaved along the (100) faces of NaCl cubes (Harshaw) were placed in a cylindrical Pyrex glass cell with a length of 11 cm and a diameter of 5 cm. Stainless steel spacers were sandwiched between the crystals so that the NaCl faces did not touch. This arrangement enabled us to interrogate 20 NaCl(100) surfaces with each face perpendicular to the incident light. Wedged silicon windows (Infrared Optical Products Inc.) were attached to both ends of the cell, and the seal between the window and the cell was made with a Viton O-ring. Tygon tubing was wrapped around the exterior of the cell and then attached to a closed cycle circulating ethylene glycol/water bath from a variable temperature unit (Neslab Instruments). This unit was used to bake the cell and crystals and maintain their temperature within  $\pm 1$  °C. The cell was attached to a vacuum line and pumped with a diffusion pump to a base pressure of  $7 \times 10^{-6}$  mbar. To ensure that the NaCl crystals were not contaminated by diffusion pump oil, a liquid nitrogen trap was placed between the cell and the pump. The cell was baked under vacuum at 100 °C for 12 h to remove air and adsorbed water. It has been shown by others<sup>29</sup> that these vacuum procedures are adequate for preparing clean NaCl(100) faces. The cell and crystals were then cooled to 24 °C, and the first isotherm was measured. Water vapor was introduced into the cell at a variety of pressures up to 19 mbar. At each pressure, measured by a Baratron gauge (MKS Instruments Inc.) accurate to  $\pm 0.1$  mbar, the adlayer of

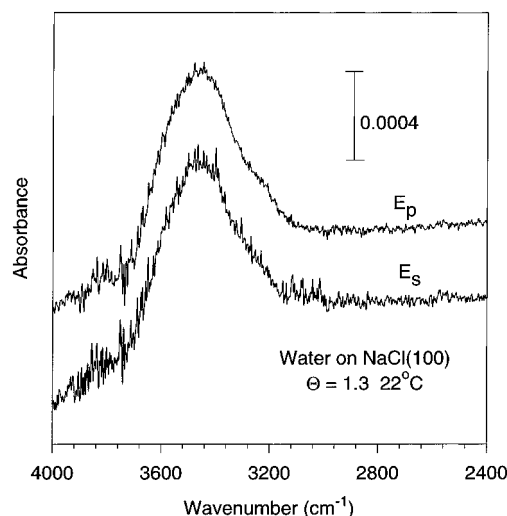


**Figure 2.** Polarized infrared spectra of water adsorbed to the NaCl(100) surface at 22 °C and at a pressure of 12.6 mbar. Spectra were obtained using the chamber represented in Figure 1.

water on the NaCl(100) face was monitored by transmission spectroscopy. The desorption of water was also spectroscopically studied while decending in pressure to explore any hysteresis effects. The cell and crystals were then rebaked. After cooling to 12 °C, the second isotherm was measured. For this isotherm the highest pressure attained was 9.0 mbar before studying the desorption process. Finally, the spontaneous dissolution of NaCl at 12 °C was observed by increasing the water pressure to 10.3 mbar, the deliquescence point of NaCl at this temperature.<sup>2</sup>

## Results

The polarized infrared spectra of  $\text{H}_2\text{O}$  on the NaCl(100) surface at 22 °C and a pressure of 12.6 mbar are shown in Figure 2. In both the  $E_p$  and  $E_s$  polarization data, a broad, almost structureless, band is present in the  $-\text{OH}$  stretching region. The frequency of the absorption is centered at  $3450 \text{ cm}^{-1}$  with a bandwidth (full width at half-maximum) of  $\Gamma = 325 \text{ cm}^{-1}$ . The integrated absorbance,  $\bar{A}$ , for the band in both  $E_s$  and  $E_p$  polarizations is  $0.35 \pm 0.03 \text{ cm}^{-1}$ . An ill-defined shoulder near  $3300 \text{ cm}^{-1}$  causes both spectra to have an asymmetric profile. Weaker, sharper features seen as fine structure in the region between 3000 and  $4000 \text{ cm}^{-1}$  are from residual gas-phase water absorption left over after the subtraction procedure. The slope on the high-frequency side of the band is an artifact of the subtraction routine. On the basis of photometric determinations, discussed in the following section, we associate the water coverage in Figure 2 with  $\Theta = 1.3 \pm 0.1$ .

A comparison between the infrared spectrum for adlayer water on NaCl(100) taken with the Pyrex cell and for a salt solution is shown in Figure 3. The top spectrum is of water adsorbed on NaCl(100) surface at 24 °C and 16 mbar with a profile indistinguishable from spectra taken with the UHV cell at a comparable pressure. The sharp features are residual water vapor absorption, and the spike at  $2950 \text{ cm}^{-1}$  is associated with an impurity within the Si windows. The lower infrared spectrum is of 5 M NaCl solution obtained from optical constants measured by Querry et al.<sup>30</sup> Spectra of both adlayer water on NaCl(100) and the salt solution show remarkable similarities in band center, band shape, and bandwidth. In the next section, we will discuss the significance of these similarities.

The frequency of the absorption band center depends on adlayer coverage as shown in Figure 4. This dependence with coverage shows similar behavior for both temperatures. There

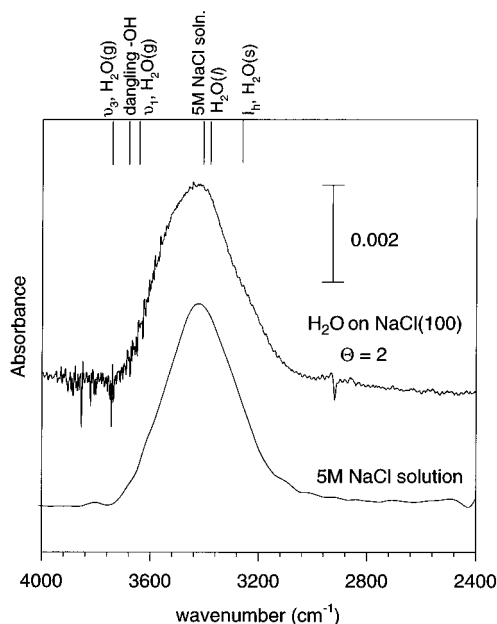


**Figure 3.** Infrared absorption of water adsorbed to NaCl(100) at 24 °C and 16 mbar (top spectrum). Bottom spectrum is the infrared absorption of 5 M NaCl solution at 27 °C obtained from optical constants in ref 30.

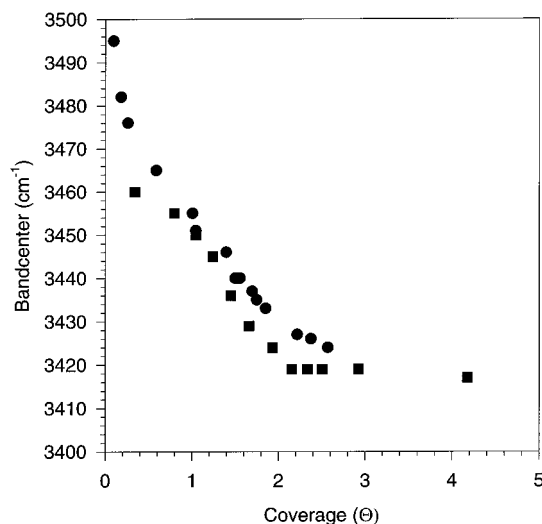


**Figure 4.** Band center change with coverage at 12 (■) and 24 °C (●).

is a sharp decrease in band center frequency from the smallest coverage measured,  $\Theta \approx 0.1$ , to  $\Theta = 2$  and then it levels off, converging to a value of  $3420 \pm 10 \text{ cm}^{-1}$  beyond  $\Theta = 3$ .

Data for the isotherms of water at 24 and 12 °C are displayed in Figure 5 with coverage as a function of pressure. At 24 °C, no absorption was observed until a pressure of 7 mbar was reached. From about 12 to 19 mbar the coverage (or more correctly integrated absorbance of the  $-\text{OH}$  stretching vibration) increases linearly with pressure as shown by the closed circles. Upon lowering the pressure, the desorption of water was evident by the decrease in absorption, represented by the open circles. Except at very low coverages, where the noise level is most troublesome, the data indicate no significant hysteresis. At 12 °C water absorption, given by closed squares, does not appear until about 3 mbar and then increases linearly from 5 to 9 mbar. After 9 mbar was reached, the pressure was lowered and the desorption monitored, as shown by the open squares. As with the 24 °C isotherm, there was little evidence of hysteresis. Moreover, the salt retained the clear, smooth appearance of the freshly cleaved surfaces. The water pressure was then increased

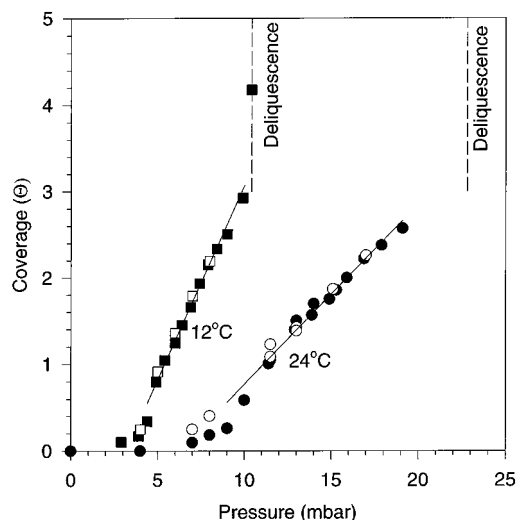


**Figure 5.** Water–NaCl(100) isotherms. (■) and (●) represent adsorptions of water as pressure is increased at 12 and 24 °C, respectively. (□) and (○) represent desorption of water as pressure is decreased at 12 and 24 °C, respectively.

again at 12 °C. Near 10 mbar there was a precipitous rise in absorption (coverage) as salt dissolution began.

## Discussion

**Spectroscopy.** We have chosen to study the adlayer of water on NaCl(100) by examining the  $-\text{OH}$  stretching vibrations (the  $\nu_1$ ,  $\nu_3$  modes) of the infrared absorption because the resulting spectroscopic signature is particularly sensitive to phase. When water condenses, the sharp lines in its vapor phase vibration–rotation spectrum centered at  $3756$  and  $3657 \text{ cm}^{-1}$ <sup>31</sup> collapse into a single diffuse absorption at  $3390 \text{ cm}^{-1}$  with full width at half-height of  $390 \text{ cm}^{-1}$ .<sup>32</sup> The solid-phase absorption ( $I_h$ -ice at  $-7$  °C) is likewise diffuse but narrower,  $260 \text{ cm}^{-1}$ , and shifted to the much lower frequency,  $3250 \text{ cm}^{-1}$ .<sup>33</sup> The coupling of molecular vibrations through hydrogen bonding is responsible for these dramatic frequency shifts.<sup>34,35</sup> For convenient comparisons, the  $-\text{OH}$  stretching frequencies of water in its various phases are shown at the top of Figure 3. The oscillator strength of the  $-\text{OH}$  stretching motions is also enhanced by an order of magnitude by the formation of hydrogen bonds.<sup>36</sup>

That the absorbance undergoes no change under interrogation by different polarizations in Figure 2 is consistent with the transition dipoles associated with  $-\text{OH}$  stretching vibrations being isotropic. (This conclusion is restricted to coverages above  $\Theta = 1$ . At lower coverages the high noise level makes accurate polarization measurements difficult.) Furthermore, there is a near match of the salt solution as well as neat liquid water absorption profiles and the spectrum of the adlayer on NaCl(100), as shown in Figure 3. These results suggest that the adsorbed phase is liquidlike or at least amorphous.

That the hydrogen-bonding arrangement of water molecules in the adlayer is changing with coverage is suggested by the band center shifts recorded in Figure 4. For the highest coverages,  $\Theta > 2$ , the band center appears to converge to value of  $3420 \pm 5 \text{ cm}^{-1}$ . Below  $\Theta = 2$  a sharp increase in band center occurs, reaching a value of  $3495 \pm 5 \text{ cm}^{-1}$  near  $\Theta = 0.1$ . The range of the frequency shift is thus  $75 \text{ cm}^{-1}$ . This is much greater than  $25 \text{ cm}^{-1}$  found for the range of concentrations in the bulk liquid. (Using the band center of  $3415 \pm 5 \text{ cm}^{-1}$  taken from Querry et al.<sup>30</sup> as presented in Figure 3 for 5 M NaCl at 27 °C and  $3395 \pm 5 \text{ cm}^{-1}$  for neat water at 27 °C from Downing and Williams,<sup>32</sup> a modest linear extrapolation gives a band center of  $3420 \pm 5 \text{ cm}^{-1}$  for the saturated salt solution at

5.4 M.<sup>2</sup>) A natural interpretation of the hydrogen-bonding arrangement of the coincident band positions of the 5.4 M salt solution and thin film water on NaCl(100) for  $\Theta > 2$  is to say that this adlayer is also a saturated solution. The frequency behavior of the low coverage adlayer,  $\Theta < 2$ , is difficult to assess, but we can note that breakup of hydrogen bonds<sup>34,35</sup> causes shifts to high wavenumber for the stretching modes moving from 3250 cm<sup>-1</sup> for ice,<sup>33</sup> 3390 cm<sup>-1</sup> for liquid water,<sup>32</sup> to 3657 cm<sup>-1</sup> ( $\nu_1$ ) and 3756 cm<sup>-1</sup> ( $\nu_3$ ) for the gas-phase molecule.<sup>31</sup> If we imagine low coverage water molecules increasingly favoring bonding to the substrate with an accompanying loss of hydrogen bonding to other water molecules, we might expect the shifts to high frequency observed in Figure 4 for  $\Theta < 2$ . For very small coverages,  $\Theta < 0.1$ , water molecules should be isolated from one another and bonded only to the substrate and sharp features correlated with  $\nu_1$  and  $\nu_3$  would be expected. We have not reached that limit in our experiments.

One feature not observed in the spectroscopy of adlayer water on NaCl(100) is an absorption feature that we can associate with dangling hydrogen vibrations. These motions would involve non-hydrogen-bonded -OH stretching vibrations of H<sub>2</sub>O molecules at the surface of the adlayer. Sum frequency generated (SFG) spectra at the air-liquid water interface show the vibrational excitation of the dangling hydrogen.<sup>37</sup> This feature, of bandwidth 100 cm<sup>-1</sup>, was found at 3700 cm<sup>-1</sup>. That we do not observe this feature does not mean there are no dangling hydrogen atoms at the surface of the adlayer; rather, it may be a consequence of the high noise level in the region near 3700 cm<sup>-1</sup> of our spectra and the differences in optical cross sections for interrogations by nonlinear SFG and linear FTIR techniques.

Building on the assumption that water adsorbed onto NaCl(100) is liquidlike, we can obtain an estimate of the adlayer coverage. We make use of a modified Beer-Lambert relationship<sup>23,25</sup> for integrated absorbance of surface species given by

$$\tilde{A} = n\bar{\sigma}S_{\text{H}_2\text{O}}/2.303 \quad (1)$$

The integrated absorbance,  $\tilde{A}$  (cm<sup>-1</sup>), of the adsorbed water was determined by numerical integration over the frequency range 3800–2950 cm<sup>-1</sup>,  $S_{\text{H}_2\text{O}}$  is the surface density of adsorbed water, and  $n$  is the number of exposed NaCl(100) faces. The integrated cross section,  $\bar{\sigma}$ , was determined from the measured, wave-number-dependent, imaginary component,  $\kappa$ , of the index of refraction,<sup>30</sup> using the equation

$$\bar{\sigma} = (4\pi/\rho) \int_{\text{band}} \kappa \tilde{\nu} d\tilde{\nu} \quad (2)$$

taken from Weis and Ewing,<sup>38</sup> where  $\rho = 3.0 \times 10^{22}$  molecules cm<sup>-3</sup> is the H<sub>2</sub>O molecular density in 5 M NaCl.<sup>2</sup> Once  $S_{\text{H}_2\text{O}}$  is calculated, the coverage,  $\Theta = S_{\text{H}_2\text{O}}/S_{\text{Na}^+\text{Cl}^-}$  is easily determined since  $S_{\text{Na}^+\text{Cl}^-}$  for the NaCl(100) face is  $6.4 \times 10^{14}$  ion pairs cm<sup>-2</sup>.<sup>2</sup>

Using this photometry procedure, we have converted all integrated absorbances to coverages,  $\Theta$ , in Figures 2–5. We realize that different hydrogen-bonding arrangements can affect  $\bar{\sigma}$  values. Had we used  $\bar{\sigma}$  for neat water<sup>32</sup> instead of 5 M NaCl, the estimate of  $\Theta$  would have differed by about 10%. For coverages less than a monolayer, values of  $\bar{\sigma}$  might be markedly different. Consequently, the coverage values we have reported are approximate. We shall examine the possible relationships between  $\Theta$  and  $\bar{\sigma}$  later.

**Isotherms.** An adlayer molecule is usually considered physically adsorbed to a surface when it can be removed, without chemical change, by simply lowering the pressure. It

is apparent from the isotherms at both temperatures that the reversible nature of water adsorption to the NaCl(100) face implies a physisorption process. Reversibility in the adsorption of water on a variety of NaCl substrates reviewed elsewhere<sup>39</sup> also supports this conclusion.

The isosteric heat of adsorption can be obtained for the high coverage phase of the adsorbed water from the integrated form of the Clausius-Clapeyron equation<sup>40</sup>

$$\ln(p_1/p_2)_\Theta = \frac{\Delta H_{\text{ads},\Theta}}{R} \left[ \frac{1}{T_1} - \frac{1}{T_2} \right] \quad (3)$$

when subscripts 1 and 2 refer to the isotherms at their corresponding pressures and temperatures. A straight line drawn through each isotherm for coverages in the range  $\Theta = 1$ –3 in Figure 5 together with eq 3 reveals  $\Delta H_{\text{ads}} = -42 \pm 1$  kJ/mol. This value compares closely with the heat of condensation of liquid water of  $\Delta H_{\text{liq}} = -44$  kJ/mol.<sup>40</sup> Again, we have evidence that the adlayer for  $\Theta > 1$  behaves like the liquid phase.

Isotherms are also valuable in describing adsorption processes because their shape often reveals information about surface-adsorbate and adsorbate-adsorbate interactions. The Langmuir isotherm smoothly rising toward monolayer saturations is a consequence of a model that neglects adsorbate-adsorbate interactions.<sup>40–42</sup> This model describes the adsorption isotherm of CO on NaCl(100) quite well,<sup>43</sup> but not H<sub>2</sub>O on NaCl(100). The quasi-chemical model<sup>42</sup> includes nearest-neighbor lateral adsorbate-adsorbate interactions and produces an isotherm that can appear as a step function.<sup>41</sup> Here there is negligible adsorption as the pressure is raised until at a critical value the coverage increases almost vertically to monolayer saturation. The isotherm shape observed for H<sub>2</sub>O on NaCl(100) under cryogenic conditions<sup>18,19</sup> and the adsorption of CH<sub>4</sub> on NaCl(100)<sup>27</sup> are well described by the quasi-chemical model. However, the isotherms of Figure 5 for the ambient H<sub>2</sub>O on NaCl(100) system bear no obvious relationship to the form of those of the quasi-chemical model. Less physically reasonable isotherms based on the Brunauer-Emmett-Teller (BET) model,<sup>40–44</sup> which admits only vertical adsorbate-adsorbate interactions, yields isotherms that can describe adsorption of C<sub>2</sub>H<sub>4</sub> on NaCl crystallites<sup>45</sup> but not H<sub>2</sub>O on NaCl(100). Even inclusion of lateral adsorbate interactions into the BET model<sup>46</sup> cannot yield isotherms of the shape we find in Figure 5. Perhaps it is not surprising that a simple adsorption model cannot explain the molecular complications available to ambient H<sub>2</sub>O on NaCl(100).

The absence of absorbance at low pressures provides a clue to the real shape of the adlayer isotherms. Consider the molecular dynamics calculations of Wasserman et al.<sup>21</sup> for submonolayer adsorption of H<sub>2</sub>O on NaCl(100). For low coverages ( $\Theta < 0.5$ ) they find adsorption of molecules on Na<sup>+</sup> with separations too great to allow hydrogen bond formation. The integrated cross section of these isolated adsorbed molecules will likely resemble that of gas-phase molecules and be much lower than water molecules that are hydrogen bonded.<sup>36</sup> Consequently, the values of  $\Theta$ , obtained from eq 2, given in the low-pressure region of Figure 5 are too low. For example, in the 24 °C experiment at 4 mbar some fraction of a monolayer is adsorbed to the NaCl(100) surface rather than the zero coverage as implied in Figure 5. A value of  $\Theta \approx 0.1$  at 7 mbar is likewise an underestimate since some of the water molecules are not hydrogen bonded. Isolated molecules adsorbed below 7 mbar are simply not detected because of their low cross section.

**Adlayer Growth.** We now draw on our spectroscopic observations of thin film water on NaCl(100) under ambient

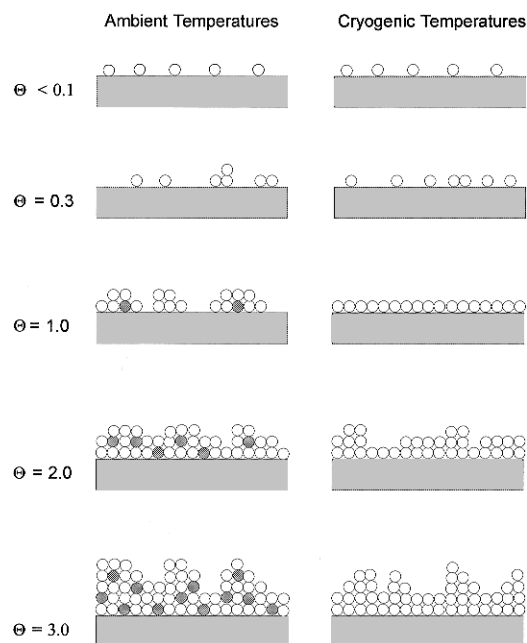


**Figure 6.** Proposed models for the growth of water adlayer on NaCl(100) at cryogenic temperatures and under ambient conditions.

conditions, together with the findings of others, to suggest a structure for the adlayer and a mechanism for its growth.

The Volmer–Weber mechanism,<sup>47</sup> where multilayer growth begins before an overlayer has completely saturated the exposed surface of the substrate, describes many aspects of water adsorption on NaCl(100) under ambient temperatures. We provide a schematic representation of this growth in the left column of Figure 6, intentionally vague in structural detail, since the experimental data offer little precise information. The open circles represent H<sub>2</sub>O molecules with no concern for their orientation. The substrate is crosshatched with its surface imagined to contain occasional steps and other defects. The crosshatched circles are either Na<sup>+</sup> or Cl<sup>−</sup> ions that have been lifted from the substrate.

At low coverages, say  $\Theta < 0.1$ , a two-dimensional lattice gas is formed. Calculations suggest that isolated adsorbed H<sub>2</sub>O molecules are attached, O-end down, over Na<sup>+</sup> surface ions with their dipoles perpendicular to the surface.<sup>21,22</sup> With this attitude, neighboring molecules cannot hydrogen bond; indeed, they tend to repel each other because of the unfavorable alignment of their dipoles.<sup>21</sup> As we have noted, our infrared spectroscopy does not detect these low coverages since the integrated cross section,  $\bar{\sigma}$ , is so small.

At some critical coverage, water molecules are forced to adsorb on adjacent sites. To facilitate their attractions within the adlayer, they tilt toward each other to participate in hydrogen bonding. As a consequence, islands form as suggested in the  $\Theta = 0.3$  panel. Since hydrogen bonding also increases  $\bar{\sigma}$ , these islands are easily detected by infrared spectroscopy. This transition from a two-dimensional lattice gas to island formation has been observed in a molecular dynamics calculation for cryogenic temperatures<sup>21</sup> and also detected as an abrupt change in surface conductivity under ambient conditions.<sup>12</sup>

As the coverage reaches  $\Theta = 1$ , we might expect that all surface sites are occupied as the islands fill in to form the monolayer. However, our infrared spectroscopy is not consistent with this result for the ambient system where we find a continuous band center frequency shift near monolayer coverage for H<sub>2</sub>O on NaCl(100). We are led to the sketch in Figure 6 for a  $\Theta = 1$  coverage. Thus, while on average  $\Theta = S_{\text{H}_2\text{O}}/S_{\text{Na}^+\text{Cl}^-} = 1$ , the coverage is not uniform. There are vacant sites

and islands of differing molecular thickness. Perhaps a few ions have been drawn into the adlayer from steps or other vacancies as suggested by others.<sup>12,14–16</sup> The variety of differing environments with coverage changes yields band center frequency shifts as well. Calculations suggesting comparable molecule–surface and molecule–molecule bond energies<sup>21</sup> are consistent with a willy-nilly growth behavior.<sup>46,48</sup>

As the coverage approaches  $\Theta = 2$ , there are more occurrences of ions now incorporated into the water thin film as solvation becomes possible. These ions, lifted from defects on the surfaces, are suggested to be the carriers responsible for surface conductivity at this adlayer coverage,<sup>12</sup> and their movement along the surface is believed to produce migration of steps.<sup>12,16,17</sup> This briny thin film does not yet have the properties of the bulk saturated salt solution since the nearby crystalline substrate still exerts a significant influence. Not until sufficient layers are formed will the properties of the film (e.g., its vapor pressure) approach those of the bulk brine solution. As coverage increases further, more possibilities become available for solvation as suggested for  $\Theta = 3$ . With the vapor pressure now approaching its deliquescence value, we suppose the liquid layer to resemble that of the saturated solution. The irregular surface for the multilayer we show in Figure 6 is qualitatively similar to that found from molecular dynamics calculations of the water liquid/vapor interface.<sup>49</sup>

We now extend our speculations of water adsorption on NaCl(100) to its growth on the cryogenic substrate as presented in the right column of Figure 6. Both theoretical considerations<sup>21</sup> and the shape of the isotherms<sup>15,19</sup> suggest a 2D gas for low coverages, say  $\Theta < 0.1$ . Abruptly at some critical coverage, suggested by molecular dynamics calculations<sup>21</sup> to be  $\Theta = 0.5$ , but arbitrarily shown as  $\Theta = 0.3$  in Figure 6, 2D island formation sets in. By  $\Theta = 1$  the monolayer is complete. (For the HAS study, this monolayer has one H<sub>2</sub>O per Na<sup>+</sup>Cl<sup>−</sup> ion pair.<sup>19</sup>) In contrast to the monolayer under ambient conditions, the cryogenic monolayer is well ordered as revealed by the sharp diffraction patterns.<sup>18,19</sup> The small differences in energy between ordered and disordered monolayer structures, which are accentuated at low temperatures, together with the entropy differences, that are reduced at lower temperatures, may account for the contrasting  $\Theta = 1$  structures in Figure 6. For the cryogenic multilayers,  $\Theta = 2$  and 3, multilayer growth proceeds by a Stranski–Krastanov mechanism.<sup>47</sup> Evidence for this growth is in the diffuse HAS scattering that sets in after the monolayer is complete. While it may be reasonable to expect that crystalline ice is forming, the surface shows irregularities as we have indicated in the  $\Theta = 2$  and 3 panels. Since ice excludes dissolved salt, we anticipate no ions trapped in the cryogenic multilayer. By contrast, the ambient multilayer is briny.

Not represented by the panels of Figure 6, which only captures a typical configuration or snapshot of structures, is the dynamic nature of the adlayer. With molecule–surface collision frequencies at a pressure of 10 mbar on the order of  $10^7 \text{ s}^{-1}$ ,<sup>40</sup> the ambient temperature adlayer structure for any coverage is undergoing submicrosecond changes in response to adsorption–desorption fluxes. Molecular dynamics calculations support this short time scale.<sup>49</sup> By contrast, for the cryogenic system, a characteristic pressure for  $-125^\circ\text{C}$  is  $10^{-8} \text{ mbar}$ <sup>19</sup> and corresponds to a scale of 100 s for the lifetime of a water molecule in the adlayer.

While we have provided some insight into the properties of adsorbed water layers on NaCl(100), many questions remain. What is the structure of the non-hydrogen-bonded sub-monolayer? What is the pH of monolayer or multilayer water

and its ability to dissolve gases or to act as a solvent for chemical reactions? What is the mechanism of dissolution? What role do defects play in the dissolution? At what temperature does the adlayer become a solid? Does this solid adlayer have more than one phase?

To provide a fuller picture of ambient thin film water on salt surfaces, other experimental techniques are needed such as sum frequency generation<sup>37</sup> and atomic force microscopy.<sup>14–19</sup> Finally molecular dynamics methods, successfully applied to surface melting,<sup>50</sup> fracturing,<sup>51</sup> and many water systems,<sup>42</sup> may perhaps be used to explore the interfacial phenomenon of dissolution. We look forward to the insight these approaches can provide.

**Acknowledgment.** This work was funded by the National Science Foundation under Grants CHE95-05892 and ATM93-31838. We have benefited from discussions with Dr. Anthony J. Stone and correspondence with Professor G. Wilse Robinson. Our thanks to Dr. Michelle Foster for her critical reading of the scientific content of the manuscript and her editorial skills.

## References and Notes

- (1) Pliny the Elder, *Natural History*; translation by H. Rackham; Harvard University Press: Cambridge, 1938; Book VIII, p 425.
- (2) National Research Council (U.S.) *International Critical Tables*, McGraw-Hill: New York, 1926.
- (3) Derjagrun, B. V.; Churaov, N. V. *Langmuir* **1987**, *3*, 607.
- (4) Vogt, R.; Finlayson-Pitts, B. J. *J. Phys. Chem.* **1994**, *98*, 3747; **1995**, *99*, 13052.
- (5) Peters, S. J.; Ewing, G. E. *J. Phys. Chem.* **1996**, *100*, 14093.
- (6) Allen, H. C.; Laux, J. M.; Vogt, R.; Finlayson-Pitts, B. J.; Heminger, J. C. *J. Phys. Chem.* **1996**, *100*, 6371.
- (7) Mason, B. J. *The Physics of Clouds*; Clarendon: Oxford, 1971.
- (8) Dash, J. G. *Films on Solid Surfaces*; Academic Press: New York, 1975.
- (9) Beaglehole, D.; Christenson, H. K. *J. Phys. Chem.* **1992**, *96*, 3395.
- (10) Hu, J.; Xias, X.-D.; Ogletree, D. F.; Salmeron, M. *Science* **1995**, *68*, 267.
- (11) de Gennes, P. G. *Rev. Mod. Phys.* **1988**, *57*, 827.
- (12) Hucher, M.; Oberlin, A.; Hobast, R. *Bull. Soc. Fr. Mineral. Crist.* **1967**, *90*, 320.
- (13) Warneck, P. *Chemistry of the Natural Atmosphere*; Academic Press: San Diego, 1988.
- (14) Shluger, A. L.; Wilson, R. M.; Williams, R. T. *Phys. Rev. B* **1994**, *49*, 4915.
- (15) Shindo, H.; Ohaski, M.; Baba, K.; Seo, A. *Surf. Sci.* **1996**, *357*–*358*, 111.
- (16) Shindo, H.; Okashi, M.; Tateishi, O.; Seo, A. *J. Chem. Soc., Faraday Trans.* **1997**, *93*, 1169.
- (17) Dai, Q.; Hu, J.; Salmeron, M. *J. Phys. Chem. B* **1997**, *101*, 1994.
- (18) Fölsch, S.; Stock, A.; Henzler, M. *Surf. Sci.* **1992**, *264*, 65.
- (19) Bruch, L. W.; Glebow, A.; Toennies, J. P.; Weiss, H. *J. Chem. Phys.* **1995**, *103*, 5109.
- (20) Heidberg, J.; Häser, W. *J. Electron Spectrosc. Relat. Phenom.* **1990**, *54/55*, 971.
- (21) Wassermann, B.; Mirbt, S.; Reif, J.; Zink, J. C.; Matthias, E. *J. Chem. Phys.* **1993**, *98*, 10049.
- (22) Jug, K.; Geudtner, G. *Surf. Sci.* **1997**, *371*, 95.
- (23) Richardson, H. H.; Chang, H.-C.; Noda, C.; Ewing, G. E. *Surf. Sci.* **1989**, *216*, 93.
- (24) Heidberg, J.; Suhren, M.; Weiss, H. *J. Electron Spectrosc. Relat. Phenom.* **1993**, *64/65*, 227.
- (25) Berg, O.; Ewing, G. E. *Surf. Sci.* **1989**, *220*, 207.
- (26) Heidberg, J.; Kampshoff, E.; Kühnemuth, R.; Schönekas, O. *J. Electron Spectrosc. Relat. Phenom.* **1993**, *64/65*, 803.
- (27) Quattrocci, L. M.; Ewing, G. E. *J. Chem. Phys.* **1992**, *96*, 4205.
- (28) Peters, S. J.; Ewing, G. E. *Langmuir*, in press.
- (29) Basssett, C. A. *Philos. Mag.* **1958**, *3*, 1042.
- (30) Querry, M. R.; Waring, R. C.; Holland, W. E.; Hale, G. M.; Nijm, W. *J. Opt. Soc. Am.* **1972**, *62*, 849.
- (31) Shimanouchi, T. *Tables of Molecular Vibrational Frequencies*; American Chemical Society: Washington, DC, 1972; Part 1, NSRDS-NBS 6.
- (32) Downing, H. D.; Williams, D. J. *Geophys. Res.* **1975**, *80*, 1656.
- (33) Warren, S. G. *Appl. Opt.* **1984**, *23*, 1306.
- (34) Pimentel, G. C.; McClellan, A. L. *The Hydrogen Bond*; Freeman: San Francisco, 1960.
- (35) Eisenberg, D. S.; Kauzmann, W. *The Structure and Properties of Liquid Water*; Oxford University Press: New York, 1969.
- (36) Ikawa, S.-I.; Maeda, S. *Spectrochim. Acta* **1968**, *24A*, 655.
- (37) Du, Q.; Freysz, E.; Shen, Y. R. *Science* **1994**, *264*, 826.
- (38) Radüge, C.; Pflumio, V.; Shen, Y. R. *Chem. Phys. Lett.* **1997**, *274*, 140.
- (39) Weis, D. D.; Ewing, G. E. *J. Geophys. Res.* **1996**, *101*, 18709.
- (40) Ewing, G. E.; Peters, S. J. *Surf. Rev. Lett.*, in press.
- (41) Atkins, P. W. *Physical Chemistry*, 5th ed.; Freeman: New York, 1994.
- (42) Adamson, A. W. *Physical Chemistry of Surfaces*, 4th ed.; John Wiley: New York, 1982.
- (43) Hill, T. L. *An Introduction to Statistical Thermodynamics*; Addison-Wesley: Reading, MA, 1960.
- (44) Noda, C.; Ewing, G. E. *Surf. Sci.* **1990**, *240*, 181.
- (45) Brunauer, S.; Emmett, H.; Teller, E. *J. Am. Chem. Soc.* **1938**, *60*, 309.
- (46) Willian, K.; Berg, O.; Ewing, G. E. *J. Chem. Soc., Faraday Trans.* **1996**, *90*, 4853.
- (47) Seri-Levy, A.; Avnir, D. *Langmuir* **1993**, *9*, 2523.
- (48) Zangwill, A. *Physics at Surfaces*; Cambridge University Press: New York, 1989.
- (49) Anastasion, N.; Fuchan, D.; Suger, K. *J. Chem. Soc., Faraday Trans. 2* **1983**, *79*, 1639.
- (50) Taylor, R. S.; Dang, L. X.; Garrett, B. C. *J. Phys. Chem.* **1996**, *100*, 11720.
- (51) Kroes, G.-J. *Science* **1992**, *275*, 365.
- (52) Lynden-Bell, R. *Science* **1994**, *293*, 1704.
- (53) Cho, C. H.; Singh, S.; Robinson, G. W. *Faraday Discuss.* **1996**, *103*, 19 and other papers cited.